

SURVEY PAPER

FRACTIONAL ADSORPTION DIFFUSION

Gerd Baumann ¹, Frank Stenger ²

Dedicated to Professor Nonnenmacher on the occasion of his 80th birthday

Abstract

The aim of this article is to generalize the diffusion based adsorption model to a fractional diffusion and fractional adsorption model. The models are formulated as nonlinear fractional boundary value problems equivalent to a singular Hammerstein integral equation. The novelty is that not only the diffusion component of the model is fractionalized but also the adsorption part. The singular Hammerstein integral equation is solved by Sinc approximations. Specific numerical schemes are presented. Based on these solutions we are able to identify different regimes of adsorption diffusion processes controlled by fractional derivatives verified by experimental data. These regimes allow to classify experiments if examined with respect to their scaling behavior.

 $MSC\ 2010$: Primary 65-XX, 45-XX, 97-XX; Secondary 65D15, 45E10, 44A35, 97N50

Key Words and Phrases: Sinc method, fractional calculus, approximation

© 2013 Diogenes Co., Sofia

pp. 737-764, DOI: 10.2478/s13540-013-0046-3

1. Introduction

The earliest examination of adsorption kinetics with control by diffusion toward a plane and an expanding sphere describing a dropping mercury electrode was examined by Delahay and coworkers [6], [7]. Later on for practical purposes radial diffusion in connection with adsorption was examined to determine pore diffusion coefficients for designing industrial equipment to be used in pollution control [10]. Due to the pollution control most studies of intraparticle diffusion have been for gas-filled porous materials because of the importance of gas-solid catalytic reactions. The subject became recently again of interest when the ideas of Delahay were used in Monte Carol simulations by Seri-Levy and Avnir [25] and generalized to a fractional formulation by Giona and Giustiniani [12] applied to fractal surfaces. In the field of nano-technology nano rods as catalyst were examined by Kwon et al [15], Such et al [29] experimentally examined diffusion and adsorption of single molecules on the KBr(001) surfaces and for bio-chemical applications like anomalous diffusion in crowded environments see [19], [9]. For recent applications on the nano scale see the compilation of Quirke [22]. The variety of applications of diffusion controlled adsorption suggests that still great interest is present in the problem. However, the modeling and solution side of the problem became settled when fractal surfaces once were introduced. In fact this geometric property was modeled by a temporal operator [12]. The temporal extension, however, opens a route to go one step further in not only generalizing the temporal properties of the diffusion equation but also by extending the temporal behavior of adsorption to a fractional modeling. First steps and formulations in this direction were given in [12]. The idea is to include memory effects into the processes. Memory effects in diffusion through non-homogeneous media have been theoretically studied by Goddard [13], who shows that this phenomenon can be represented by introducing memory kernels and convolution integrals in time to describe the history effects arising from microscopic diffusional relaxation [12]. It turned out in these studies that the experimentally important quantity M_t/M_{∞} is represented in an implicit analytic way. As already mentioned the model discussed in [12] was restricted to absorption on a fractal surface. The adsorption process itself was assumed to be normal. In general such an assumption can be extended to a fractional adsorption process. One of the aims of this article is to generalize not only the diffusion process to a fractional process but also the adsorption process can be included in such a scheme. Another target of this article is to overcome the complicated analytic calculations especially of the inverse Laplace transform, if at all possible, by a numeric approach delivering high accurate results for the experimentally important quantity M_t/M_{∞} . The used numeric method does not only show an exponential convergence but is also able to deal with singularities. Singularities show up in fractional models as soon as we introduce fractional integral or differential operators [2]. However, the used approximation method, the Sinc method, is able to deal with such kind of obstacles effectively in all kind of calculations [28].

The paper is organized as follows. In Section 2 we formulate the problem. Section 3 introduces the different normal and fractional models for diffusion controlled adsorption. It turns out that all these models can be formulated as a nonlinear integral equation a so called Hammerstein equation. Section 4 discusses the numerical solution of Hammerstein equations by applying Sinc approximations to it. The explicit collocation formulas based on Laplace techniques are given. Section 5 presents some numerical examples for normal and fractional diffusion controlled adsorption models. The final section summarizes and discusses the results.

2. Problem Formulation

Let us assume we are examining spherical beads of finite size allowing a substance to diffuse and become adsorbed on the surface of the beads. One of the assumptions of the model now is that a chemical is diffusing in a finite d-dimensional spherical space governed by the radial diffusion equation. The diffusion in a d-dimensional spherical space is usually described by the diffusion equation in spherical coordinates as

$$\partial_t u(t,r) = \frac{1}{r^{d-1}} \frac{\partial}{\partial r} \left(r^{d-1} \frac{\partial u(t,r)}{\partial r} \right), \tag{1}$$

here d represents the dimension of the space; i.e. $d = 1, 2, 3, \ldots$ This kind of equation can be generalized to a fractional version of the form

$$\mathcal{D}_{0,t}^{\mu}u(t,r) = \frac{1}{r^{d-1}}\frac{\partial}{\partial r}\left(r^{d-1}\frac{\partial u(t,r)}{\partial r}\right) \quad \text{with} \quad 0 < \mu \le 1.$$
 (2)

Such kind of equation was discussed by Metzler et al. [20] in connection with anomalous diffusion. However, the authors did not consider the equation in connection with boundary conditions. We will use this equation but add to the initial conditions boundary conditions of the problem. The boundary conditions we will add, assume that there is a temporal change of the diffusing substance on the surface. Moreover these surface interaction is governed by a generic non-linear interaction. The boundary conditions we assume for the diffusion process are

$$u(t,1) = b(y(t)) \quad \text{for} \quad t > 0 \tag{3}$$

which is a time dependent nonlinear generic function b(y) on the surface with y = y(t) a time dependent function at the normalized radius r = 1. For the function b(y) there exist several empirical models used in adsorption theory known as Langmuir, Henry, Freundlich, Sip, or Troth's model to mention only a few; for a detailed discussion see [8]. Relation (3) is also known as the adsorption isotherm. The diffusion process satisfies at the origin the conditions

$$\frac{\partial u(t,0)}{\partial r} = 0, \quad t > 0 \tag{4}$$

and

$$u(0,r) = 0 \text{ for } 0 < r < 1.$$
 (5)

This means that the diffusing quantity u(t,r) is vanishing everywhere in the domain and its first order derivative is finite at the origin. In addition the assumed adsorption process is governed at the surface with r=1 by adsorption rate equation

$$\frac{dy(t)}{dt} = -\alpha \frac{\partial u(t,1)}{\partial r} \tag{6}$$

with initial condition $y(0) = y_0$. Relation (6) is nothing more than Fick's first law on the surface. The model of this diffusion and adsorption process assumes that due to the fractional processes in the fluid the process of diffusion will be changed to an anomalous behavior. The adsorption process in (6) is assumed to follow the Fickian law with an integer rate of change in time. However, this model is under question by different authors and some call it even "inadequate" [31], [1], [30]. It is worth noting that while some of the models are able to explain various features they fail, with few exceptions, to account for rather consistently recorded characteristics. This situation is the reason to generalize the rate of change from an integer value to a fractional adsorption rate governed by the equation

$$\mathcal{D}_{0,t}^{\gamma} y(t) = -\alpha \frac{\partial u(t,1)}{\partial r} \quad \text{with} \quad 0 < \gamma \le 1.$$
 (7)

The fractional model of adsorption assumes that the rate of adsorption is determined by the gradient of the diffusing quantity at the boundary of the region. This however means that we assume the existence of a first kind fractional Fick law on the surface.

We will first examine the normal adsorption process (Fickian) in one, two and three dimensions to establish a reference model. Afterwards we discuss the influence of fractional diffusion and the influence of fractional adsorption on the solution. Finally we will combine both fractional diffusion and fractional adsorption in a common model.

3. Adsorption Models

3.1. Normal Adsorption in 1, 2 and 3 Dimensions

The adsorption problem with diffusion originally given as a boundary value problem can be re-written to a nonlinear integral equation of Volterra type using a difference kernel. To have a model let us assume that a chemical is diffusing in a restricted space governed by the radial diffusion equation

$$\partial_t u(t,r) = \beta \left(\frac{\partial^2 u}{\partial r^2} + \frac{d-1}{r} \frac{\partial u}{\partial r} \right) \quad \text{with} \quad 0 < r < 1, t > 0, \text{ and } d = 1, 2, 3$$
(8)

satisfying the nonlinear boundary conditions

$$u(t,1) = b(y(t)) \quad \text{for} \quad t > 0 \tag{9}$$

$$\frac{\partial u(t,0)}{\partial r} = 0, \ t > 0 \tag{10}$$

and the initial condition

$$u(0,r) = 0 \text{ for } 0 < r < 1.$$
 (11)

In addition, let us assume that there is an adsorption process governed at the surface of the restricted region with radius r=1 described by

$$\frac{\mathrm{dy}(t)}{\mathrm{dt}} = -\alpha \frac{\partial u(t,1)}{\partial r} \tag{12}$$

with initial condition $y(0) = y_0$.

The procedure to convert this system of boundary and initial conditions to an integral equation goes as follows. First Laplace transform equations (8) to (10) and (12). From these transforms the following equations follow in the Laplace space

$$su(s,r) = \beta \left(u'' + \frac{d-1}{r}u' \right), \tag{13}$$

$$u(s,1) = b(s), \tag{14}$$

$$u'(s,0) = 0. (15)$$

Depending on the dimension of the space the Laplace transformed representation of the solution and the derivative has different representations. The solution for the different dimensions are given below.

For d=1

$$u(s,r) = \frac{b(s)e^{\frac{\sqrt{s}}{\sqrt{\beta}} - \frac{r\sqrt{s}}{\sqrt{\beta}}} \left(e^{\frac{2r\sqrt{s}}{\sqrt{\beta}}} + 1\right)}{e^{\frac{2\sqrt{s}}{\sqrt{\beta}}} + 1},$$
(16)

for d=2

$$u(s,r) = \frac{b(s)J_0\left(\frac{ir\sqrt{s}}{\sqrt{\beta}}\right)}{J_0\left(\frac{i\sqrt{s}}{\sqrt{\beta}}\right)}$$
(17)

where $J_0(x)$ is Bessel's zeroth order function. In case of d=3,

$$u(s,r) = \frac{b(s)e^{\sqrt{\frac{s}{\beta}} - r\sqrt{\frac{s}{\beta}}} \left(e^{2r\sqrt{\frac{s}{\beta}}} - 1\right)}{r\left(e^{2\sqrt{\frac{s}{\beta}}} - 1\right)}.$$
 (18)

For r=1, we have the condition for the first order derivative for d=1

$$u'(s,1) = \frac{\sqrt{s} \left(e^{\frac{2\sqrt{s}}{\sqrt{\beta}}} - 1 \right) b(s)}{\sqrt{\beta} \left(e^{\frac{2\sqrt{s}}{\sqrt{\beta}}} + 1 \right)},\tag{19}$$

d=2

$$u'(s,1) = -\frac{i\sqrt{s}b(s)J_1\left(\frac{i\sqrt{s}}{\sqrt{\beta}}\right)}{\sqrt{\beta}J_0\left(\frac{i\sqrt{s}}{\sqrt{\beta}}\right)},\tag{20}$$

with $J_0(x)$ and $J_1(x)$ Bessel's function of order zero and one. The derivative at the boundary for d=3 is

$$u'(s,1) = \left(\frac{\sqrt{s}\left(e^{\frac{2\sqrt{s}}{\sqrt{\beta}}} + 1\right)}{\sqrt{\beta}\left(e^{\frac{2\sqrt{s}}{\sqrt{\beta}}} - 1\right)} - 1\right)b(s)$$
 (21)

which is the right hand side of the absorption equation (12). Laplace transformation of this equation then delivers

$$sy(s) - y_0 = -\alpha u'(s, 1) = -\alpha \mathcal{K}(s)b(s)$$
(22)

with K(s) the Laplace factor of the equation following from expressions (19), (20), and (21) for the different dimensions, respectively. Finally the determining equation in Laplace space reads

$$sy(s) - y_0 = -\alpha \mathcal{K}(s)b(s), \tag{23}$$

or prepared to invert the Laplace transform

$$y(s) - \frac{y_0}{s} = -\alpha \frac{1}{s} \mathcal{K}(s)b(s) = -\alpha k(s)b(s). \tag{24}$$

The right hand side represents a convolution in Laplace space while the left hand side is the representation of the first derivative. Inverting

the Laplace transform results formally to the nonlinear Volterra integral equation (Hammerstein equation) of second kind

$$y(t) = y_0 - \alpha \int_0^t K(t - \tau)b(y(\tau))d\tau.$$
 (25)

The representation of the Hammerstein integral equation assumes that the inversion of the kernel and the nonlinearity is possible. For a simplified kernel Gavrilyuk et al derived such kind of equation and demonstrated the existence and uniqueness of a continuous and non increasing solution [11]. However, in most of the cases the explicit representation of K is rarely possible. Thus the kernel is not known as an explicit function of t. This lack of knowledge is a real obstacle in analytic solutions of (25) [3]. In addition the analytic inversion might be not possible due to the nonlinearity of the function b. However, for practical applications it is frequently sufficient to know a numerical approximation of the Hammerstein equation (25). To find such a reasonable approximation of (25), we use Sinc methods allowing us to solve the singular Hammerstein equation. It turns out that it is sufficient at this stage to know the Laplace representation of the kernel because the Sinc approximation of the convolution integral in (25) is actually based on a Laplace representation and separation of the integrand [2]. To demonstrate that Sinc methods are not only useful for boundary value problems but also for the fractional formulation of such kind of boundary value problems we introduce different fractional variants of the original model in the following sections.

3.2. Fractional Diffusion and Normal Adsorption

For a model with fractional diffusion and normal adsorption the assumption is that the diffusion takes place in a limited space where the temporal motion is governed by a fractional derivative of Liouville-Riemann or Caputo type [4], [14]. The origin of such kind of diffusion can be either a crowded environment as in cells [9], [2] or the result of a continuous time random walks [24]. However, the spatial diffusion is still formulated using ordinary differentiation. The fractional diffusion in a spherical beat is thus given by

$${}^{C}\mathcal{D}^{\mu}_{0,t}u(t,r) = \beta \left(\frac{\partial^{2} u}{\partial r^{2}} + \frac{d-1}{r}\frac{\partial u}{\partial r}\right) \text{ with } 0 < r < 1, \ 0 < \mu < 1, \text{ and } t > 0,$$
(26)

satisfying the nonlinear boundary and initial conditions given in equations (9) to (12).

The procedure to convert this system of equations, boundary conditions, and initial condition to an integral equation is the same as for the case discussed in Section 3.1. First Laplace transform equation (26). From this transform the following equations follow in Laplace space

$$s^{\mu}u(s,r) - s^{\mu-1}u(0,r) = \beta\left(u'' + \frac{2}{r}u'\right)$$
 (27)

which simplifies due to the initial value of u(0,r)=0 to

$$s^{\mu}u(s,r) = \beta\left(u'' + \frac{2}{r}u'\right). \tag{28}$$

The remaining boundary conditions given by (14) and (15) are used to solve the two point boundary value problem (28). This boundary value problem in Laplace space has for the different dimensions d the solution: for d = 1

$$u(s,r) = \frac{b(s)e^{\frac{s^{\mu/2}}{\sqrt{\beta}} - \frac{rs^{\mu/2}}{\sqrt{\beta}}} \left(e^{\frac{2rs^{\mu/2}}{\sqrt{\beta}}} + 1\right)}{e^{\frac{2s^{\mu/2}}{\sqrt{\beta}}} + 1},$$
(29)

d = 2

$$u(s,r) = \frac{b(s)J_0\left(\frac{irs^{\mu/2}}{\sqrt{\beta}}\right)}{J_0\left(\frac{is^{\mu/2}}{\sqrt{\beta}}\right)},\tag{30}$$

and d=3

$$u(s,r) = \frac{b(s)e^{\sqrt{\frac{s^{\mu}}{\beta}} - r\sqrt{\frac{s^{\mu}}{\beta}}} \left(e^{2r\sqrt{\frac{s^{\mu}}{\beta}}} - 1\right)}{r\left(e^{2\sqrt{\frac{s^{\mu}}{\beta}}} - 1\right)}.$$
 (31)

For the surface of the beat at r=1 we derive the condition for the first order derivative used in (12) to describe the adsorption process for dimension

d = 1

$$u'(s,1) = \frac{b(s)s^{\mu/2} \left(e^{\frac{2s^{\mu/2}}{\sqrt{\beta}}} - 1\right)}{\sqrt{\beta} \left(e^{\frac{2s^{\mu/2}}{\sqrt{\beta}}} + 1\right)},$$
(32)

d = 2

$$u'(s,1) = -\frac{ib(s)s^{\mu/2}J_1\left(\frac{is^{\mu/2}}{\sqrt{\beta}}\right)}{\sqrt{\beta}J_0\left(\frac{is^{\mu/2}}{\sqrt{\beta}}\right)},\tag{33}$$

and d=3

$$u'(s,1) = \left(b(s)\left(e^{2\sqrt{\frac{s^{\mu}}{\beta}}}\left(\sqrt{\frac{s^{\mu}}{\beta}} - 1\right) + \sqrt{\frac{s^{\mu}}{\beta}} + 1\right)\right) / \left(e^{2\sqrt{\frac{s^{\mu}}{\beta}}} - 1\right). \tag{34}$$

The Laplace transformation of equation (12) and incorporating the initial condition for this equation then delivers

$$sy(s) - y_0 = -\alpha u'(s, 1) = -\alpha \mathcal{K}(s)b(s)$$
(35)

which simplifies to

$$y(s) - \frac{y_0}{s} = -\alpha \frac{1}{s} \mathcal{K}(s)b(s) = -\alpha k(s)b(s). \tag{36}$$

The right hand side represents a convolution in Laplace space while the left hand side is the representation of the function and its initial condition. Inverting the Laplace transform results again to the nonlinear Hammerstein equation

$$y(t) = y_0 - \alpha \int_0^t K(t - \tau)b(y(\tau))d\tau. \tag{37}$$

Here the singular kernel includes a complicated relation of the fractional behavior of the diffusion process. However, the type of Volterra integral equation is the same as derived in Section 3.1 but with a changed kernel given by (36). Again it is not important to know the temporal behavior of the kernel because the Laplace representation of the kernel will be used in the Sinc approximation. A similar extension to a fractional equation of the original equations can be done by introducing fractional derivatives into equation (12) on the left hand side. We will skip this sub model in the presentation here and go to the combination of both fractional models in a common model in the next section.

3.3. Fractional Diffusion and Fractional Adsorption

For such a combination of fractal models let us assume that not only the diffusion process is a fractional process but also the interaction of the chemicals with the adsorption surface. This means that we replace the adsorption relation (12) by its fractional representation using a Caputo derivative. In this extended model relation (12) reads

$${}^{C}\mathcal{D}_{0,t}^{\gamma}y(t) = -\alpha \frac{\partial u(t,1)}{\partial r}$$
(38)

with initial condition $y(0) = y_0$. The boundary and initial conditions are the same as before. So that we can use the conversion process in Laplace space as discussed. The solution of the diffusion boundary problem is given by (29) to (34). What actually changes is the Laplace transform of the

fractional adsorption equation becoming in Laplace space the representa-

$$s^{\gamma} y(s) - s^{\gamma - 1} y_0 = -\alpha u'(s, 1) = -\alpha \mathcal{K}(s) b(s). \tag{39}$$

So that finally the determining equation is

$$y(s) - \frac{y_0}{s} = -\alpha \frac{1}{s^{\gamma}} \mathcal{K}(s)b(s) = -\alpha k(s)b(s)$$
(40)

with $k(s) = \mathcal{K}(s)/s^{\gamma}$. The right hand side represents again a convolution in Laplace space while the left hand side is a representation of the function and its initial value. Inverting the Laplace transform results to the nonlinear Hammerstein integral equation

$$y(t) = y_0 - \alpha \int_0^t K(t - \tau)b(y(\tau))d\tau. \tag{41}$$

As a result in all approaches to generalize the diffusion adsorption process to a fractional diffusion and fractional adsorption model we end up with a nonlinear second kind Hammerstein integral equation. The differences of the models are encoded in the structure of the kernel which includes the total information about the underlying physical and chemical processes.

In the next section we will discuss how to solve such Hammerstein integral equations via use of Sinc indefinite convolution [28], Section 1.5.9. We mention, in passing that an alternative method of solution is also possible by applying the inverse Laplace transform procedure of [28], Section 1.5.10, to the above derived Laplace transform identities. However, we will not pursue this alternative procedure in this paper.

4. Sinc Methods for Hammerstein Integral Equations

In this section we introduce the Sinc representation of the Hammerstein integral equation. An extensive discussion of the solution of singular integral equations is available in [2]. The analytic solution of Hammerstein integral equations (HIE) are extensively discussed by Brunner [3]. We start out from the HIE introduced in the last section. This type of equation can be generally written as

$$y(t) = g(t) - \alpha \int_0^t K(t - \tau)b(y(\tau))d\tau, \tag{42}$$

where $K(t-\tau)$ is a difference kernel and b(y) represents a generic nonlinear function of the unknown y. The external function g(t), we introduce here, simplifies in the adsorption models to a constant. We note that the kernel $K(\tau)$ has different representations according to the models discussed in Section 3.

Sinc methods originally introduced by Frank Stenger [18], [26], [28] use a Cardinal approximation based on shifted Sinc functions collocated by conformal maps [26]. The major idea of a Sinc approximation is to use a conformal map ϕ and its inverse $\psi(z) = \phi^{-1}(z)$ to generate so called Sinc points $z_n = \psi(nh)$ where $h = \pi / \sqrt{N}$ is the step length and m = 2N + 1 the total number of Sinc points. The Sinc approximation of a function is then given by

$$f(x) \approx \sum_{k=-N}^{N} f(x_k) \operatorname{sinc}\left(\frac{\phi(x) - kh}{h}\right) = \boldsymbol{V}_m(f).\boldsymbol{w}_m$$
 (43)

with $V_m(f) = (f(x_{-N}), \ldots, f(x_N))^T$ a vector of discrete function values and \boldsymbol{w}_m a collection of basis functions $\boldsymbol{w}_m = \left(\operatorname{sinc}\left(\frac{\phi(x)+Nh}{h}\right), \ldots, \operatorname{sinc}\left(\frac{\phi(x)-Nh}{h}\right)\right)$. $\phi(z)$ is the conformal map for a finite or infinite interval [26]. Convolution integrals of the type (37) can be approximated by Sinc methods as follows [27]. For collocating a convolution integral and for obtaining explicit approximations of a functions p defined by

$$p(x) = \int_{a}^{x} f(x - t)g(t)dt \text{ with } x \in (a, b),$$
 (44)

where x is part of an finite interval $(a,b) = \Gamma \subseteq \mathbb{R}$, unless otherwise indicated. Before we start to present the collocation of equation (44) we mention that there is a special approach to evaluate the convolution integrals by using a Laplace transform. In fact, Lubich [16], [17] introduced this way of calculation by the following idea

$$p(x) = \int_0^x f(x - t)g(t)dt = \frac{1}{2\pi i} \int_{\mathcal{C}} \widehat{f}(s) \int_0^x e^{st} g(x - t)dtds \qquad (45)$$

for which the inner integral solves the initial value problem y' = sy + g with g(0) = 0. We assume that the Laplace transform (Stenger-Laplace transform)

$$\widehat{f}(s) = \int_{E} f(t)e^{-t/s}dt \tag{46}$$

with E any subset of \mathbb{R} such that $E \supseteq (0, b - a)$, exists for all $s \in \Omega^+ = \{s \in \mathbb{C} | \Re(s) > 0\}$. In this notation we get

$$p = \widehat{f}(\mathcal{J})g \approx \widehat{f}(\mathcal{J}_m)g \tag{47}$$

which is an accurate approximation, at least for g in a certain space [28]. The procedure to calculate the convolution integrals is now as follows. The collocated integral $\mathcal{J}_m = \boldsymbol{w}_m A_m \boldsymbol{V}_m$, upon diagonalizing of A_m in the form

$$A_m = X_m.\text{diag}[s_{m,-M}, \dots, s_{m,N}].X_m^{-1}$$
 (48)

with $\Sigma = \text{diag}[s_{-M}, \dots, s_N]$ as the eigenvalues arranged in a diagonal matrix for each of the matrices A_m . Then the Stenger-Laplace transform (46) delivers the square matrices $\hat{f}(A_m)$ defined via the equations

$$\hat{f}(A_m) = X_m . \operatorname{diag}\left[\hat{f}(s_{m,-M}), \dots, \hat{f}(s_{m,N})\right] . X_m^{-1} = X_m \hat{f}(\Sigma) . X_m^{-1}.$$
 (49)

Thus the approximation of (47) is given by

$$\widehat{f}(\mathcal{J})g \approx \widehat{f}(\mathcal{J}_m) g = \boldsymbol{w}_m \cdot \widehat{f}(A_m) \boldsymbol{V}_m(g) = \boldsymbol{w} \cdot X_m \widehat{f}(\Sigma) \cdot X_m^{-1} \cdot \boldsymbol{V}_m(g).$$
 (50)

This formula delivers a finite approximation of the convolution integrals p. The convergence of the method is exponential as was proved by Stenger [27]. Using (44) as basis we know now how to collocate (37) by applying Sinc methods. The approximation of equation (37) follows from

$$y + \widehat{f}(\mathcal{J})b(y) = g \iff V_m(y) + \widehat{f}(A_m)\boldsymbol{V}_m(b(y)) = \boldsymbol{V}_m(g),$$
 (51)

representing a non-linear system of equations for the unknowns $\boldsymbol{V}_m(y)$

$$\boldsymbol{V}_{m}(y) + \widehat{f}(A_{m}) \cdot \boldsymbol{V}_{m}(b(y)) = \boldsymbol{V}_{m}(g)$$
(52)

which based on (49) has the detailed representation

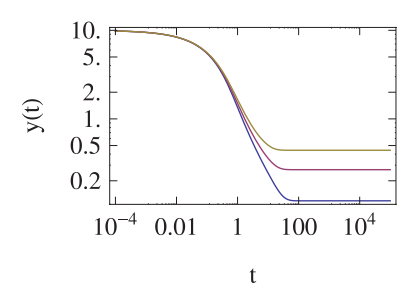
$$\boldsymbol{V}_{m}(y) + X_{m}.\operatorname{diag}\left[\widehat{f}\left(s_{m,-M}\right),\ldots,\widehat{f}\left(s_{m,N}\right)\right].X_{m}^{-1}.\boldsymbol{V}_{m}(b(y)) = \boldsymbol{V}_{m}(g).$$
(53)

If the integral operator \mathcal{J} in (52) is defined for (0,T), then the norm of A_m is proportional to T, and hence the IE use a contraction for all T sufficiently small, so that the IE can then be solved using successive approximation. We note that the approximation $\mathbf{V}_m(b(y))$ is accurate under the assumption that b(z) is analytic on an interval that contains the solution y. Analyticity directly implies that we get exponential convergence for y, [28], [26].

Equation (53) represents a non-linear system of equations for the unknowns $V_m(y)$. The diagonal matrix diag[] includes the discrete Laplace transform at the eigenvalues of A_m . This matrix is the key to solve the HIE creating the separation of kernel and nonlinearity. In addition the use of the Laplace representation of the kernel avoids to derive the explicit representation of the kernel in original variables. This feature is an important key in the solution of nonlinear boundary value problems based on Sinc methods. Solving the system (53) delivers the coefficients for a Sinc approximation of the function y by

$$y(t) \approx \boldsymbol{w}_m.\boldsymbol{V}_m(y). \tag{54}$$

This approximation again shows exponential convergence, [27].



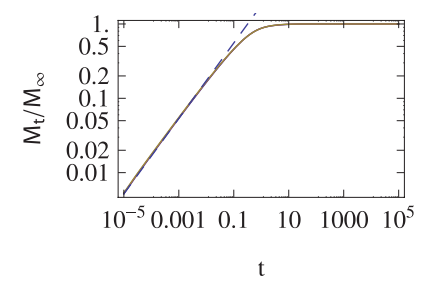


FIGURE 1. Solution of the HIE equation using the nonlinearity $b(y) = y/(1+y^{3/4})$, $\alpha = 1$, $\beta = 10^{-2}$, and $y_0 = 10$. The number of Sinc points m = 129. Shown are the solutions for the 1,2, and 3 dimensional case (bottom up on the right side of the graph, left panel). The right panel shows the normalized ratio M_t/M_{∞} experimentally accessible. The asymptotic slope (dashed line) for small times for all dimensions is $M_t/M_{\infty} \sim t^{1/2}$ expected for a diffusion governed process.

5. Examples

The following examples demonstrate the application of Sinc methods to HIE in connection with the fractional and non-fractional adsorption diffusion problem.

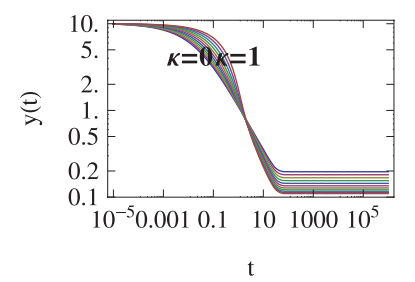
5.1. Normal Adsorption in 1, 2 and 3 Dimensions

Using the approximation scheme (52) we are able to derive the solution for y(t). To be more specific we fix the parameters and functions in the model [17] by

$$\alpha = 1, \beta = 10^{-1}, y_0 = 10, \text{ and } b(y) = y / (1 + y^{3/4}),$$
 (55)

where b(y) represents a Redlich-Peterson isotherm [23]. Under these conditions we solved equation (37) by a Sinc approximation. The results of the approximation are shown in Figure 1. We observe that for all dimensions there exist a stable value y_{∞} . This value and the initial value is used to define the experimental accessible quantity $M_t/M_{\infty} = (y(t) - y_0) / (y_{\infty} - y_0)$. This quantity is also known as the total amount of diffusing substance entering or leaving the sphere [5].

We observe that there is a common scaling region of the approximation of y for all dimensions around 1. However, for increasing dimension we observe that the substances on the surface become constants after a



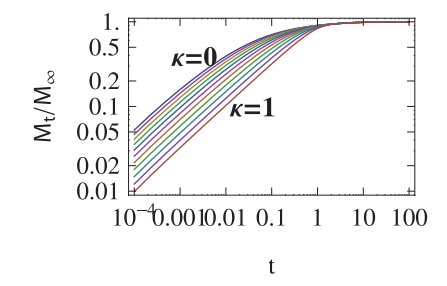
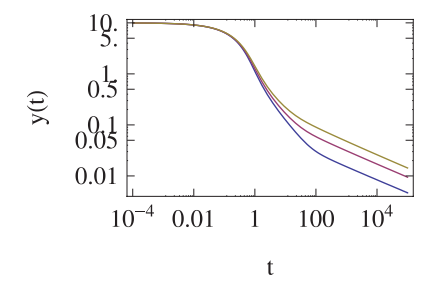


FIGURE 2. Influence of the nonlinearity on the scaling behavior of M_t/M_{∞} . The exponent κ of the nonlinearity $y/(1+y^{\kappa})$ was changed in the range $\kappa \in [0,1]$ in steps of $\delta \kappa = 1/10$. It is obvious from the graph (right panel) that the nonlinearity does not change the scaling behavior of the model. There is only a shift but not a change in the scaling exponent. The calculation were carried out for the 1 dim. case with $\alpha = 1$, $\beta = 10^{-2}$, and $y_0 = 10$. The number of Sinc points in the calculation is m = 129. The asymptotic slope for small times for $M_t/M_{\infty} \sim t^{1/2}$ as expected for a diffusion governed process.

time of $t \approx 10-30$. This means that saturation sets in. The adsorption process becomes saturated at different levels for each dimension. In a real experiment there is no access to measure the temporal change of concentration y in the solution. However, the experimental accessible quantity is the total amount of the diffusing substance. Since the process in the pores of the beat are completely diffusion controlled we expect that this quantity changes as $M_t/M_{\infty} \sim t^{1/2}$ accordingly. The quantity M_t/M_{∞} corresponds to the mean deviation of a diffusion process. The determination of the scaling factor κ by means of a linear regression of the double logarithmic data delivers in fact that $\eta \approx 0.5072\ldots$ which is in agreement with the theoretical expectation.

We checked also the influence of the nonlinearity for the adsorption process to the scaling region of M_t/M_{∞} . For this reason we changed the exponent in $b(y) = y/(1+y^{\kappa})$ in the region $0 \le \kappa \le 1$. $\kappa = 0$ corresponds to a linear model known as Henry's model while $\kappa = 1$ represents the Langmuir model. The observation is using the same parameters as before there is no change of the scaling exponent. Only a shift in the log-log plot is introduced in y. The results are shown in Figure 2.



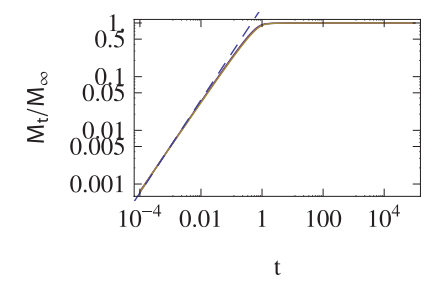


FIGURE 3. Solution of the HIE equation using the nonlinearity $b(y) = y/(1+y^{3/4})$, $\alpha = 1$, $\beta = 10^{-2}$, $\mu = 1/3$ and $y_0 = 10$. The number of Sinc points m = 129. Shown are the solutions for the 1,2, and 3 dimensional case (bottom up left panel). The right panel shows the total amount of diffusing substance entering or leaving the sphere. The scaling exponent of $M_t/M_{\infty} \sim t^{0.8647}$ is $\eta = 0.8647...$ which is different from the normal diffusion controlled model.

The results demonstrate that the calculations are consistent with theoretical expectations of diffusion controlled adsorption processes. In addition we note that there is no influence of the nonlinearity on the scaling exponent.

5.2. Fractional Diffusion and Normal Adsorption

For this type of model we examined the fractional diffusion in the d-dimensional sphere with normal adsorption on the surface. The calculations are shown in a double logarithmic plot in Figure 3. The left panel shows y as a function of time while the right panel shows the total amount of the diffusing substance M_t/M_{∞} in a double logarithmic plot.

The result of the approximation is that a fractional diffusion changes the asymptotic behavior for all dimensions in the same way. Instead of a constant value we observe a scaling region over several decades for y. The scaling region of the three solutions sets in at $t \approx 20-100$. While the higher dimensions start earlier with the scaling the one dimensional model starts later. However, for all three dimensions the scaling exponent of the solution y is numerically the same with a scaling exponent of about $\delta \approx 0.71517...$ For short times the total amount of the diffusing substance M_t/M_{∞} shows also a scaling region over several decades. Here the scaling exponent for the specific choice of parameters is $\eta \approx 0.8647...$ larger than the scaling exponent for a normal diffusion $\eta = 1/2$.

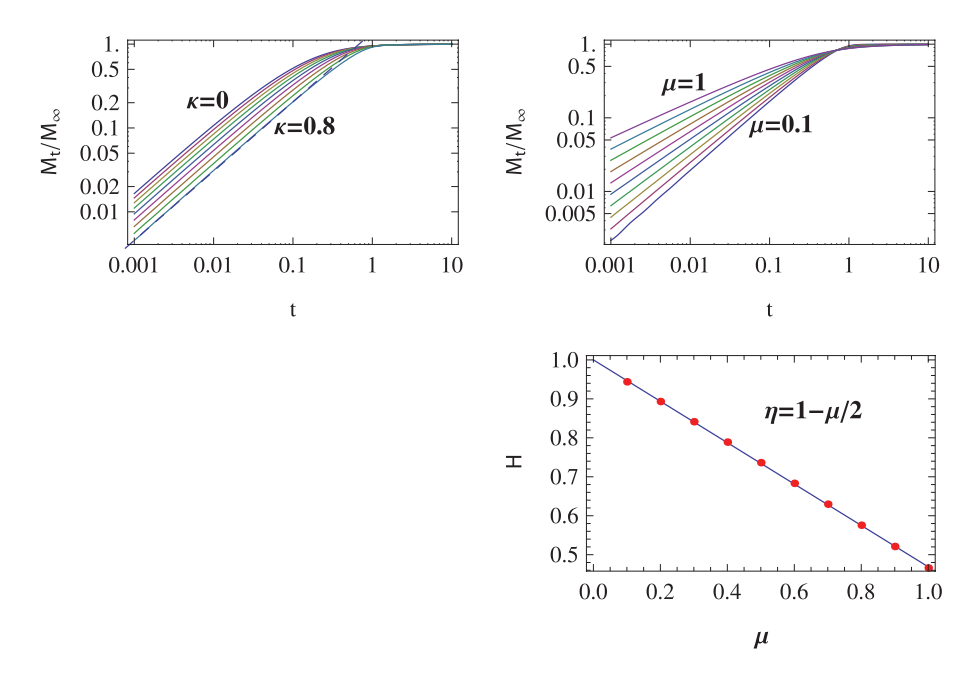
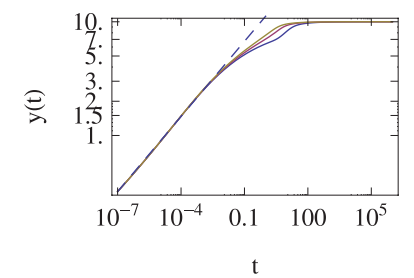


FIGURE 4. Scaling behavior of the fractional model if we change the nonlinear exponent κ and the fractional differentiation order. From top left panel where κ is changed we conclude that a change in the nonlinear interaction has no influence on the scaling behavior of M_t/M_{∞} here $\eta=0.8256$ is always constant. If we change the fractional differentiation order μ (right top panel) we observe a linear change of the scaling exponent $\eta=1-\mu/2$.

For fractional diffusion we also checked the change of the scaling if we change the nonlinearity parameter κ and the fractional differentiation order μ . The results are shown in Figure 4. The top row shows the scaling behavior if we change κ (left panel) and μ (right panel). The bottom row shows the scaling exponents η if we change the fractional differentiation order μ . The graph shows that $\eta = 1 - \mu/2$ is connected by a linear relation. This is consistent with the limit $\mu \to 1$ delivering $\eta = 1/2$ for a normal diffusion.

The numerically derived relations are in accordance with the scaling exponents discussed for fractional diffusion processes. In addition we note that the type of nonlinear adsorption process does not affect the scaling behavior of fractional diffusion. The derived results are consistent with the discussion given in literature [20].



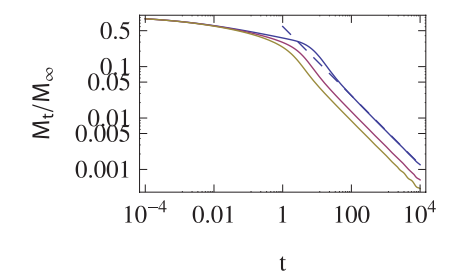
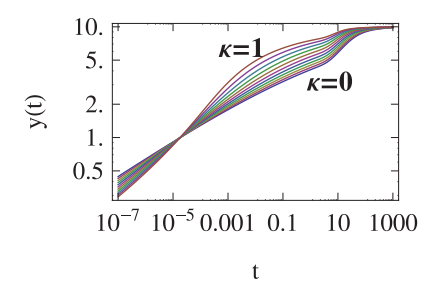


FIGURE 5. Solution of the HIE equation using the nonlinearity $b(y) = y/(1+y^{3/4})$, $\alpha = 1$, $\beta = 10^{-2}$, $\gamma = 1/3$ and $y_0 = 10$. The number of Sinc points m = 129. Shown are the solutions for the 1,2, and 3 dimensional case (bottom up left panel). The right panel shows the experimentally accessible quantity $M_t/M_{\infty} \sim t^{-0.6724}$ representing the same asymptotic behavior for all three dimensions.

5.3. Normal Diffusion and Fractional Adsorption

This model examines a fractional adsorption process controlled by a normal diffusion in a d-dimensional sphere. The approximations for y and M_t/M_{∞} are shown in a double logarithmic plot in Figure 5. The 1 dim. case is represented by the lower curve while the 3 dim. case is given by the top curve. For the 1 dim. diffusion model we observe a dip before the saturation of the adsorption at the pre-specified level of $y_0 = 10$. The dip for the 1 dim. case occurs around $t \approx 1$. For short times $t \ll 1$ there is a common scaling region extending over several decades. The common slope for all three dimensions is $\delta = 0.22031...$ represented in Figure 5 by a dashed line (left panel) to demonstrate the asymptotic behavior for short times. The solutions were generated by a finite integration on the domain $t \in [0, 10^6]$. On the left panel we calculated the total amount of the diffusing substance. The log-log plot shows that for large times there exists a scaling region extending over several decades. The scaling exponent for this region is $\eta \approx -0.6724...$ Although the curves are separated for each dimension the slope of the scaling region is the same.

The change of the nonlinearity as before was checked again. We observe that the solution y itself changes in a certain way. However, the quantity M_t/M_{∞} keeps the same scaling behavior with the same scaling exponent for the different nonlinearity parameters κ . This again demonstrates that the adsorption diffusion model is insensitive with respect to the change of nonlinearity. This is only true for the experimentally accessible value M_t/M_{∞} but not for the solution y (see Figure 6).



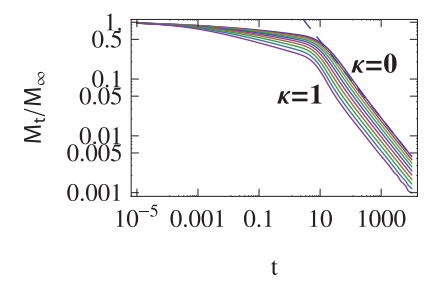


FIGURE 6. Variation of the nonlinear exponent κ for purely fractional adsorption. Parameters for the calculation are $b(y) = y/(1+y^{\kappa})$, and $\kappa \in [0,1]$, $\alpha = 1$, $\beta = 10^{-2}$, $\gamma = 1/3$, and $y_0 = 10$. The number of Sinc points m = 259. The right panel shows the experimentally accessible quantity $M_t/M_{\infty} \sim t^{-0.6789}$ representing the same asymptotic behavior (dashed line) for all variations of the nonlinearity.

We also examined the influence of the fractional dimension on the scaling exponent of M_t/M_{∞} . For this reason we changed $\gamma \in [0, 1/2]$ the results of the calculations are shown in Figure 7. For $\gamma > 1/2$ the same scaling behavior is observed so that the total range for γ is $0 \le \gamma \le 1$. Again we determined the relation between η and γ following the relation $\eta = \gamma - 1$ (see Fig. 7 bottom right).

5.4. Fractional Diffusion and Fractional Adsorption

This fourth example considers a fractional diffusion and a fractional adsorption at the same time. The solution of the complete fractional model is shown in Figure 8. Since there are two processes competing the fractional diffusion and the fractional adsorption we have to distinguish the cases $\mu > \gamma$, $\mu < \gamma$, and $\mu = \gamma$. The three cases are arranged from top left, top right to bottom left. Examples for a specific choice of values are shown in Figure 8. In Figure 9 we show for the same choice of parameters for the measurable quantity M_t/M_{∞} .

The solutions y shown in Figure 8 are that for $\mu > \gamma$ (top left) there is no scaling region in y for the adsorbed quantity. In case that $\mu < \gamma$ we observe for large times a scaling behavior with a common scaling factor independent of the geometric dimension of the model. However, there is also a region for small times where saturation sets in. This is also observed in the calculations with equal fractional exponents $\mu = \gamma$. An example with equal exponents $\mu = \gamma$ is shown in Figure 8 lower left panel. The total amount of the diffusing substance M_t/M_{∞} is shown in Figure

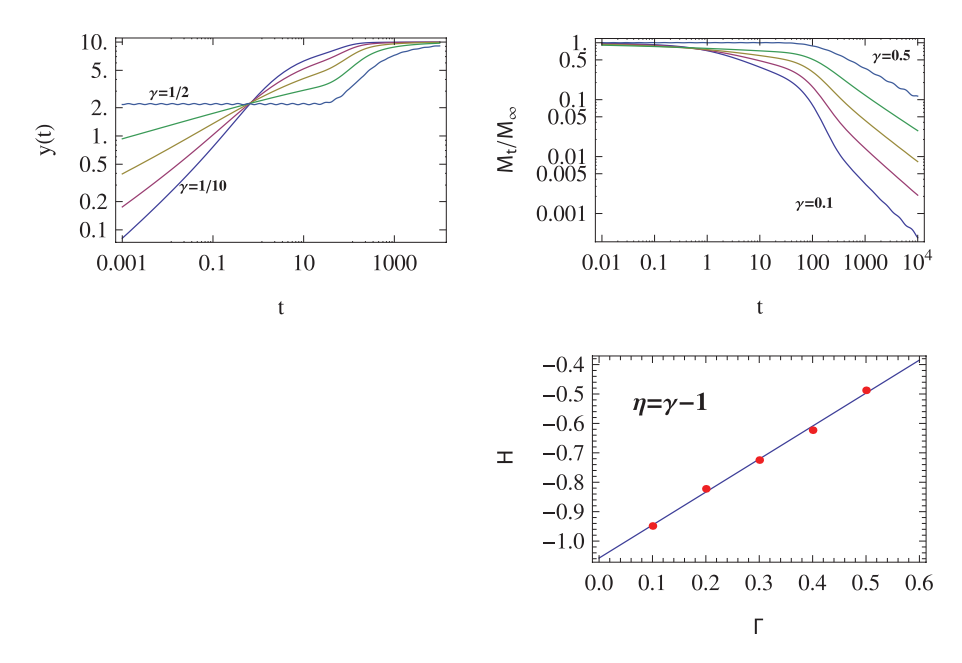
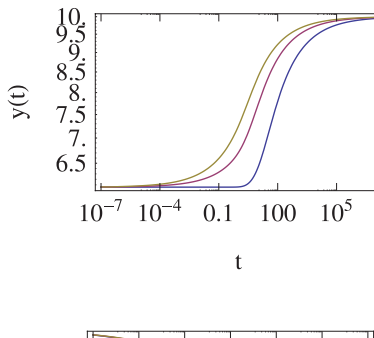
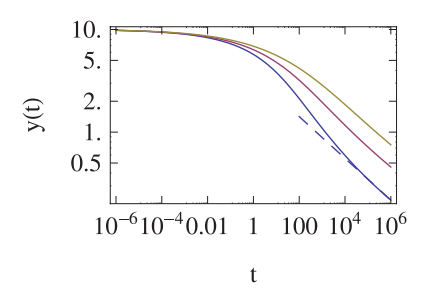


FIGURE 7. Variation of the fractional derivative γ for purely fractional adsorption. Parameters for the calculation are $b(y) = y/(1+y^{3/4})$, and $\alpha = 1$, $\beta = 10^{-2}$, $\gamma \in [0,1/2]$, and $y_0 = 10$. The number of Sinc points m = 259. The right panel shows the experimentally accessible quantity $M_t/M_{\infty} \sim t^{-\eta}$.

9. We measured for the three different cases of fractional differentiation choices three different scaling exponents. This observation encouraged a more detailed examination for the three different cases $\mu > \gamma$, $\mu = \gamma$, and $\mu < \gamma$. The calculations for these cases are shown in Figures 10 to 12. Since μ and γ can be changed independently with the constraint $0 \le \gamma \le 1/2$ we expect that there exists a relation among the scaling exponents η , μ , and γ . These relations were derived by numerical calculations similar to the one shown in Figures 10 to 12. A summary of the derived relations is given in Figure 13. Figure 13 shows that we have to distinguish three regions for the choice of μ and γ . For each of these regions there exists a scaling relation different from the others. Specifically we found that for $\mu > \gamma$ the scaling relation is $\eta = \gamma - \mu$, for equal orders of fractional derivatives $\mu = \gamma$ we find $\eta = \gamma/2$, and for $\mu < \gamma$ the relation is given by $\eta = 2\gamma - \mu$. These scaling relations are numerically represented in the lower right panel of Figures 10 to 12 for a specific choice of μ . The range for the fractional differentiation





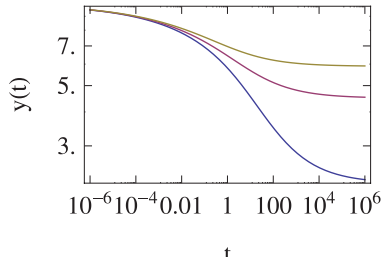
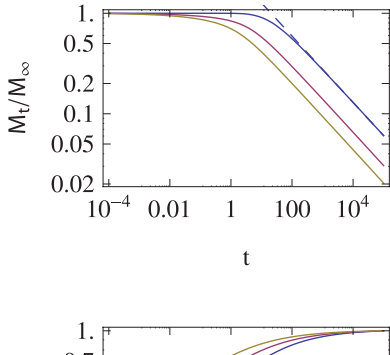
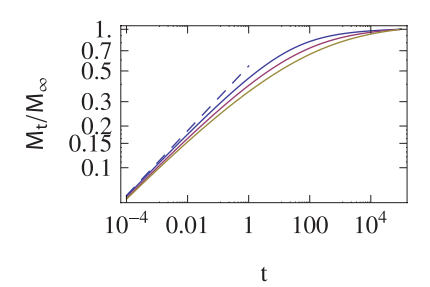


FIGURE 8. Solution of the HIE equation using the nonlinearity $b(y) = y/(1+y^{3/4})$, $\alpha = 1$, $\beta = 10^{-2}$, $y_0 = 10$, and $\mu = 2/3$, $\gamma = 1/3$ left panel, and $\mu = 1/5$, $\gamma = 1/3$ right panel. Panel left bottom shows the solution for $\mu = \gamma = 1/3$ the other choices for parameters are the same as before. The number of Sinc points is m = 257. Shown are the solutions for the 1, 2, and 3 dimensional case (bottom up in each graph). The dashed line indicates that the asymptotic scaling behavior follows a law $y \sim t^{-1/5}$ which is the same for all dimensions.

order is in all cases $0 \le \mu, \gamma \le 1$. However, in Figures 10 to 12, only a subset of this range is shown.

The results about scaling are summarized in Figure 13. The graph and the table of Figure 13 collect information about the different scaling regimes of an adsorption diffusion process governed by two fractional derivatives μ and γ . We detected in our calculations three regimes for the selection of μ and γ . For all regimes we found that $0 \le \mu, \gamma \le 1$ including the normal adsorption diffusion process with $\mu = \gamma = 1$. The three different regimes are $\mu < \gamma, \mu = \gamma$, and $\mu > \gamma$. Each of these regimes possesses a characteristic scaling law of the quantity $M_t/M_{\infty} \sim t^{\eta}$. The scaling exponent η is a function of the fractional derivatives tabulated in Figure 13. For $\mu < \gamma$ we found $\eta = 2\gamma - \mu$, for $\mu = \gamma$ the relation $\eta = \gamma/2$ exists, and for





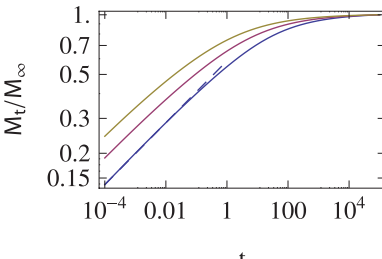


FIGURE 9. The total amount of the diffusing substance M_t/M_{∞} using the nonlinearity $b(y) = y/(1+y^{3/4})$, $\alpha=1$, $\beta=10^{-2}$, $y_0=10$, and $\mu=2/3$, $\gamma=1/3$ left panel, and $\mu=1/5$, $\gamma=1/3$ right panel. Panel left bottom shows the solution for $\mu=\gamma=1/3$ the other parameter choices are the same as before. The number of Sinc points is m=257. Shown are the solutions for the 1,2, and 3 dimensional case (bottom up). The dashed lines indicate that the asymptotic scaling behavior follows a law $M_t/M_{\infty} \sim t^{\eta}$ which is the same for all dimensions. The scaling exponent η is given for the different fractional differentiation orders by $\eta=-0.33\ldots$, $\eta=0.233\ldots$, and $\eta=0.1561$ for the panels from top to bottom and left to right, respectively.

 $\mu > \gamma$ the scaling exponent η is given by $\eta = \gamma - \mu$. If we apply a similar classification given for diffusion processes by Metzler and Klafter [21] to adsorption diffusion processes, we can distinguish four different cases. For $\mu < \gamma$ we can classify based on the magnitude of η the following cases super adsorption diffusion processes for $\eta > 1/2$, sub adsorption diffusion for $\eta < 1/2$, and normal adsorption diffusion for $\eta = 1/2$. However, there is a region where η becomes negative which we call negated adsorption diffusion. According to this classification we can identify different regions in the $\mu\gamma$ -plane corresponding to these regimes. For $\mu > \gamma$ there exists a

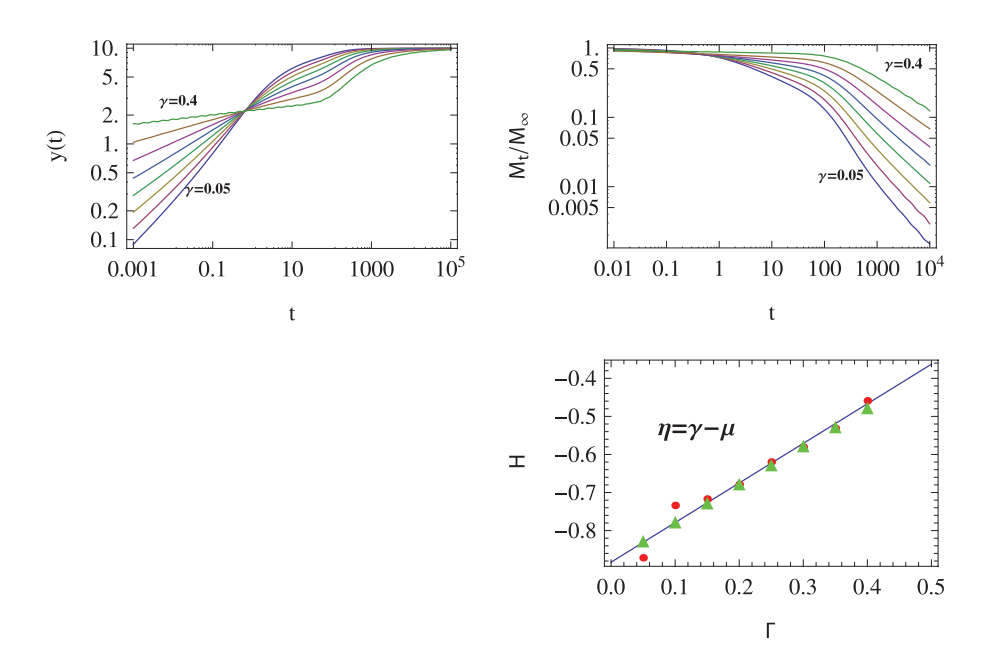


FIGURE 10. The solution and the total amount of the diffusing substance M_t/M_{∞} using the nonlinearity $b(y) = y/(1+y^{3/4})$, $\alpha = 1$, $\beta = 10^{-2}$, $y_0 = 10$, and $\mu = 7/8$, $\gamma \in [.05, 7/8]$ in steps of 0.05. The lower panel shows the relation for $\gamma < \mu$ as $\eta = \gamma - \mu$. The dots are the scaling exponents determined from the calculations. Triangles use the formula $\eta = \gamma - \mu$ based on the given data for γ . The number of Sinc points is m = 257.

single domain while for $\mu < \gamma$ we have three sub domains (see Figure 13). In addition the case $\mu = \gamma$ separates these domains.

5.5. Experimental Observations

To check the outlined fractional adsorption diffusion model we analyzed a set of data taken from [31]. The experimental setup is concerned with adsorption in polymeric composites. The data was acquired from Fig. 1 and Fig. 2 of [31] by digitizing the plots and reading the records from this digital version. The data acquisition was done on a screen of 1280×800 pixels resolution. Thus the gained data are not of high accuracy but serve to test the validity of the model. Since the time domain of the data recording is limited to a finite range we used the available data and derived an estimation of the scaling exponents for these data. The normalization of the experimental data also limited the range to the unit interval with a

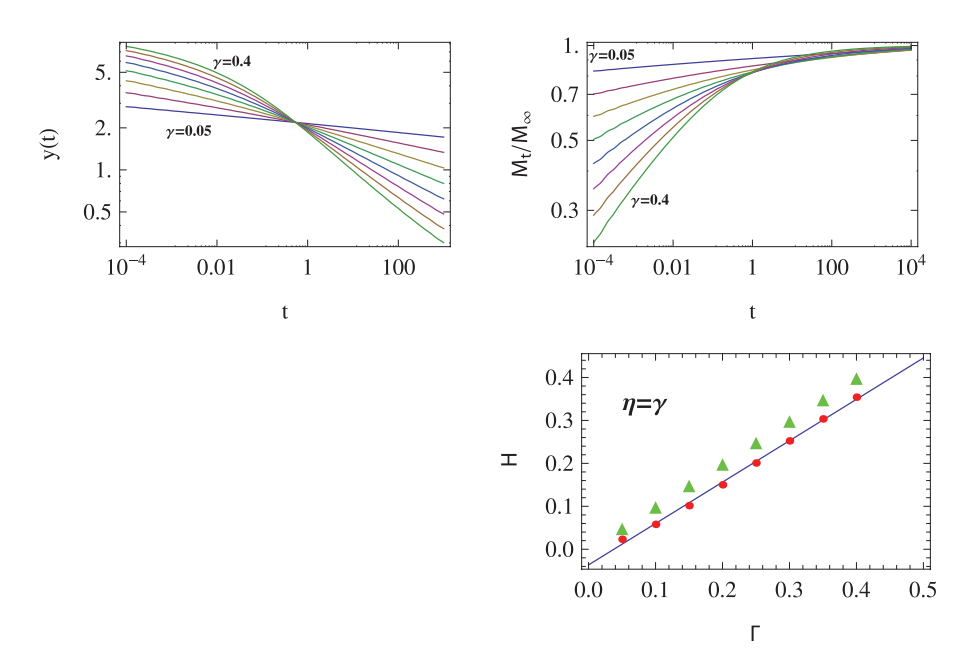


FIGURE 11. The solution and the total amount of the diffusing substance M_t/M_{∞} using the nonlinearity $b(y) = y/(1+y^{3/4})$, $\alpha = 1$, $\beta = 10^{-2}$, $y_0 = 10$, and $\mu = \gamma$, $\gamma \in [.05, 0.4]$ in steps of 0.05. The lower panel shows the relation for $\gamma = \mu$ as $\eta = \gamma$. The dots are the scaling exponents determined from the calculations. Triangles use the formula $\eta = \gamma$ based on the given data for γ . The number of Sinc points m = 129.

lower resolution point. These limitations must be taken into account if we interpret the derived results. However, we verified the scaling behavior of our calculated solutions at very small times delivering nearly the same asymptotic slope as was estimated for larger time intervals. The results of our fitting are shown in Figure 14. The experimentally determined scaling behavior is indicated in all plots by dashed lines.

Knowing the scaling exponents we used the classification given in Figure 13 to fix the diffusion type. Since we have positive slopes we are on the diagonal or below the diagonal line of the phase diagram. Assuming that both fractional exponents are the same we have sub-diffusive processes. On the other hand if we assume that $\mu < \gamma$ then we have super diffusion. In both cases we are able to fix the differentiation orders μ and γ according the relations given in Figure 13. In all cases the experimental scaling exponents are reproduced. The alignment of data points on the theoretical curve

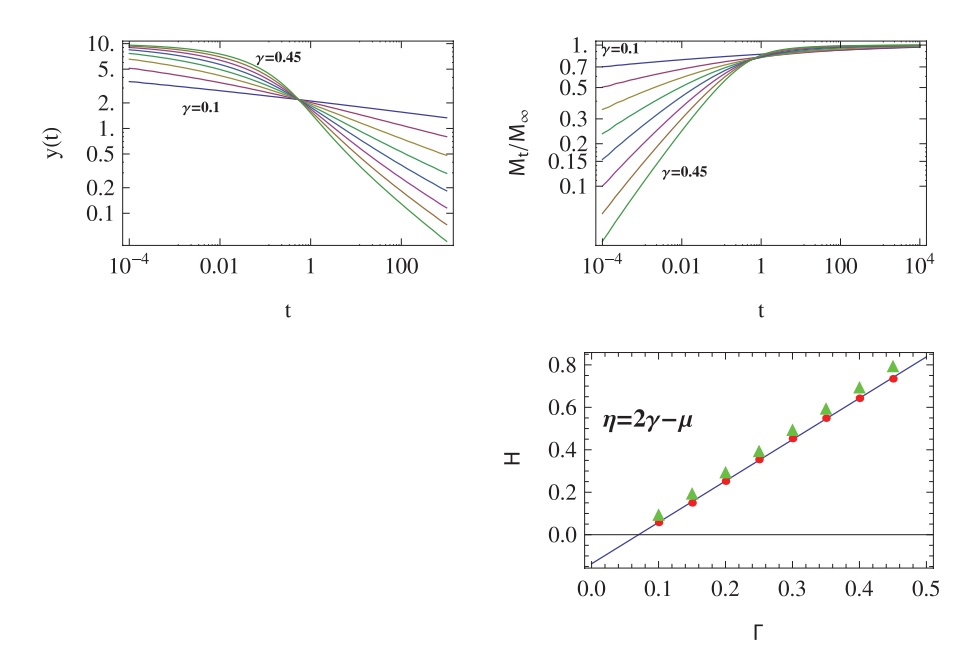


FIGURE 12. The solution and the total amount of the diffusing substance M_t/M_{∞} using the nonlinearity $b(y) = y/(1+y^{3/4})$, $\alpha = 1$, $\beta = 10^{-2}$, $y_0 = 10$, and $\mu = 1/10$, $\gamma \in [.1, 0.45]$ in steps of 0.05. The lower panel shows the relation for $\mu < \gamma$ as $\eta = 2\gamma - \mu$. The dots are the scaling exponents determined from the calculations. Triangles use the formula $\eta = 2\gamma - \mu$ based on the given data for γ . The number of Sinc points m = 129.

is consistent. However, the selection of the fractional exponents is not unique. There exist a variety of choices delivering the same exponent. At the moment we are not able to distinguish which of these parameter selections is the most appropriate one. Comparing theory with experiment we can of course minimize the deviation of both but this does not resolve the selection procedure of fractional derivatives.

6. Conclusions

We demonstrated that a fractional adsorption diffusion process can be modelled by a fractional diffusion equation and a fractional Fick law on the surface. The combined model is equivalent to a Hammerstein integral equation with a nonlinear kernel representing the adsorption isotherm.

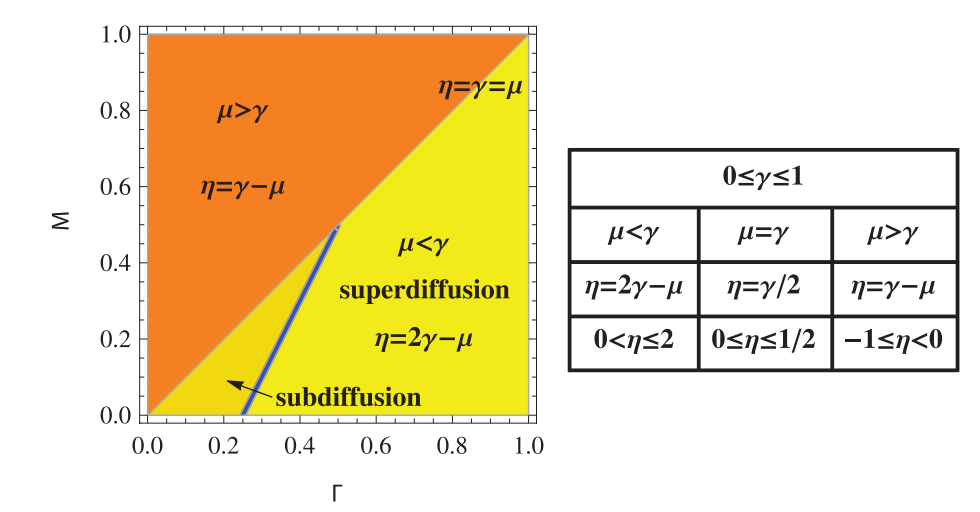


FIGURE 13. Classification of diffusion regimes. Shown are three specific combinations of fractional derivative orders for μ and γ . The cases are tabulated in the table on the right. The ranges for μ and γ are $0 \le \mu, \gamma \le 1$. The major cases are $\mu > \gamma$, $\mu = \gamma$, and $\mu < \gamma$. For each region we derived the scaling law for $M_t/M_{\infty} \sim t^{\eta}$. The different cases correspond to $\mu > \gamma$ with $\eta = \gamma - \mu$, for $\mu = \gamma$ we find $\eta = \gamma/2$, and for $\mu < \gamma$ we have $\eta = 2\gamma - \mu$. If we apply the classification of diffusion processes [21], we can identify normal diffusion, sub diffusion and super diffusion, as well as a non classified regime. Super adsorption diffusion is represented by the yellow region. Sub adsorption diffusion occurs in the brown region and normal adsorption diffusion is given by the separation line between the yellow and brown region. The orange region represents a non-classified region in the scheme of diffusion processes. We will call it negated adsorption diffusion because the slope changes its sign.

The model is solvable by using Sinc methods in connection with Stenger-Laplace transforms. The explicit numerical schemes are given to determine the numerical approximation based on collocation. A classification of the different models demonstrate that different kind of diffusion processes are connected with fractional adsorption.

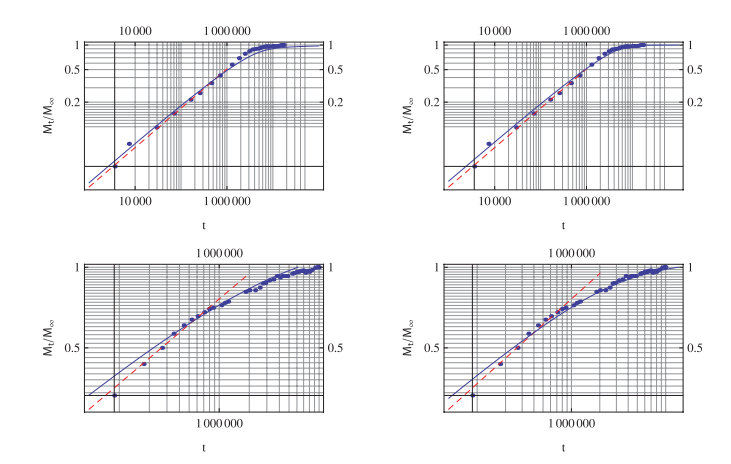


Figure 14. Experimental evaluation of the fractional adsorption diffusion model by two sets of data taken from [31] Fig. 1 and Fig. 2, respectively. The data were measured on Uni-directional AS4/3501—6 gr/ep coupons in sea water at 23°C (top) and 50°C (bottom). For estimating the scaling exponents the first eleven records were used starting at record two. These sets of data delivered scaling exponents $\eta_{23} = 0.48$ and $\eta_{50} = 0.31$, respectively. The solid lines were calculated based on equations (2) and (7). Since the equations are scaled the solid lines are invariant with respect to scaledings of the time and M_t/M_{∞} scales. Left column $\mu < \gamma$ and right column with $\mu = \gamma$. The parameters for the fractional model are as follows: $\mu = \gamma$: $\mu = \gamma = 0.96$ (top), $\mu = \gamma = 0.62$ (bottom). $\mu < \gamma$: $\mu = 0.85$, $\gamma = 0.905$ (top) super diffusion , $\mu = 0.25$, $\gamma = 0.441$ (bottom) subdiffusion.

References

- [1] A. Apicella, L. Nicolais, G. Astarita, and E. Drioli, Hygrothermal history dependence of moisture sorption kinetics in epoxy resins. *Poly. Eng. Sci.* **21** (1981), 18–22.
- [2] G. Baumann and F. Stenger, Fractional calculus and Sinc methods. *Fract. Calc. Appl. Anal.* **14**, No 4 (2011), 568–622; DOI: 10.2478/s13540-011-0035-3; http://link.springer.com/journal/13540/.
- [3] H. Brunner, Collocation Methods for Volterra Integral and Related Functional Differential Equations. Cambridge University Press, Cambridge (2004).

- [4] M. Caputo and F. Mainardi, A new dissipation model based on memory mechanism. *Pure Appl. Geophys.* **91** (1971), 134–147.
- [5] J. Crank, *The Mathematics of Diffusion*. Oxford Univ. Press, Oxford (2009).
- [6] P. Delahay and I. Trachtenberg, Adsorption kinetics and electrode processes. J. Amer. Chem. Soc. 79 (1957), 2355–2362.
- [7] P. Delahay and Ch.T. Fike, Adsorption kinetics with diffusion controlthe plane and the expanding sphere. *J. Amer. Chem. Soc.* **80** (1958), 2628–2630.
- [8] D.D. Do, Adsorption Analysis. Imperial College Press, London (1998).
- [9] Z. Földes-Papp and G. Baumann, Fluorescence molecule counting for single-molecule studies in crowded environment of living cells without and with broken ergodicity. Cur. Pharm. Biot. 12 (2011), 824–833.
- [10] M. Friedrich, A. Seidel, and D. Gelbin, Measuring adsorption rates from an aqueous solution, *AIChE J.* **31** (1985), 324–327.
- [11] I.P. Gavrilyuk, P.F. Zhuk, and L.N. Bondarenko, Some inverse problems of internal-diffusion kinetics of adsorption. J. Math. Sci. 66 (1993), 2387–2390.
- [12] M. Giona and M. Giustiniani, Adsorption kinetics on fractal surfaces. J. Phys. Chem. 100 (1996), 16690–16699.
- [13] J.D. Goddard, History effects in transient diffusion through heterogeneous media. *Ind. Chem. Res.* **31** (1992), 713–721.
- [14] A.A. Kilbas, H.M. Srivastava, and J.J. Trujillo, *Theory and Applications of Fractional Differential Equations*. Elsevier, Amsterdam (2006).
- [15] T. Kwon, M. Min, H. Lee, and B.J. Kim, Facile preparation of water soluble CuPt nanorods with controlled aspect ratio and study on their catalytic properties in water. J. Mater. Chem. 21 (2011), 11956–11960.
- [16] C. Lubich, Convolution quadrature and discretized operational calculus: I. Numer. Math. **52** (1988), 129–145.
- [17] C. Lubich, Convolution quadrature and discretized operational calculus: II. *Numer. Math.* **52** (1988), 413–425.
- [18] J. McNamee, F. Stenger, and E.L. Whitney, Whittaker's cardinal function in retrospect. *Math. Comp.* **23** (1971), 141–154.
- [19] Y. Meroz, I.M. Sokolov, J. Klafter, Subdiffusion of mixed origins: When ergodicity and nonergodicity coexist. *Phys. Rev. E* 81 (2010), 010101-1-010101-4.
- [20] R. Metzler, W.G. Glöckle, and Th. Nonnenmacher, Fractional model equation for anomalous diffusion. *Physica A* **211** (1994), 13–24.
- [21] R. Metzler and J. Klafter, The random walk's guide to anomalous diffusion. *Phys. Rep.* **339** (2000), 1–77.

- [22] N. Quirke, Adsorption and Transport at the Nanoscale. CRC/Taylor & Francis, Boca Raton, Fla. (2006).
- [23] O.J. Redlich and D.L. Peterson, A useful adsorption isotherm. J. Phys. Chem. **63** (1959), 1024–1024.
- [24] H. Scher and E.W. Montroll, Anomalous transit-time dispersion in amorphous solids. *Phys. Rev. B* **12** (1975), 2455–2477.
- [25] A. Seri-Levy and D. Avnir, Kinetics of diffusion-limited adsorption on fractal surfaces. J. Phys. Chem. 97 (1993), 10380–10384.
- [26] F. Stenger, Numerical Methods Based on Sinc and Analytic Functions. Springer, New York (1993).
- [27] F. Stenger, Collocating convolutions. Math. Comp. 64 (1995), 211–235.
- [28] F. Stenger, Handbook of Sinc Numerical Methods. CRC Press, Boca Raton (2011).
- [29] B. Such, Th. Trevethan, Th. Glatzel, Sh. Kawai, L. Zimmerli, E. Meyer, A.L. Shluger, C.H.M. Amijs, and P. Mendoza, Functionalized truxenes: adsorption and diffusion of single molecules on the KBr(001) surface. ACS Nano 4 (2010), 3429–3439.
- [30] Y.J. Weitsman, A continuum diffusion model for viscoelastic materials. J. Phys. Chem. **94** (1990), 961–968.
- [31] Y.J. Weitsman and Ya-J. Guo, A correlation between fluid-induced damage and anomalous fluid sorption in polymeric composites. Comp. Sci. Tech. **62** (2002), 889–908.
- ¹ Mathematics Department, German University in Cairo New Cairo City, EGYPT and

Department of Mathematical Physics, University of Ulm Albert-Einstein-Allee 11

D-89069 Ulm, GERMANY

Received: January 16, 2013 e-mail: Gerd.Baumann@GUC.edu.eg,

Gerd.Baumann@physik.uni-ulm.de

² School of Computing, University of Utah 3414 Merrill Engineering Bldg. Salt Lake City, UT 84112, USA e-mail: Sinc_f@msn.com , stenger@cs.utah.edu

Please cite to this paper as published in:

Fract. Calc. Appl. Anal., Vol. 16, No 3 (2013), pp. 737–764; DOI:10.2478/s13540-013-0046-3